Non-nearest neighbour ICD in clusters

2016 New J. Phys. 18 043028

(http://iopscience.iop.org/1367-2630/18/4/043028)

New Journal of Physics
The open access journal at the forefront of physics

Deutsche Physikalische Gesellschaft DPG
IOP Institute of Physics

Published in partnership with: Deutsche Physikalische Gesellschaft and the Institute of Physics

OPEN ACCESS

RECEIVED
9 December 2015

REVISED
17 March 2016

ACCEPTED FOR PUBLICATION
23 March 2016

PUBLISHED
19 April 2016

PAPER

Non-nearest neighbour ICD in clusters

E Fasshauer

Centre for Theoretical and Computational Chemistry, Department of Chemistry, University of Tromsø—The Arctic University of Norway, N-9037 Tromsø, Norway

E-mail: elke.fasshauer@uit.no

Keywords: interatomic coulombic decay, neon clusters, NeAr clusters, lifetimes, bulk and surface atoms, decay widths, icosahedral versus cuboctahedral structure

Abstract

Interatomic Coulombic decay (ICD) is an electronic decay process of excited, ionized systems. It has been shown to occur in a multitude of small and large systems. The effects of more than one possible decay partner are discussed in detail illustrated by simulated ICD electron spectra of NeAr clusters and pure Ne clusters. Hereby, the mostly underestimated contribution of decay with non-nearest neighbours is highlighted. In the neon clusters, the lifetime of the bulk atoms is found to be in excellent agreement with experiment (Jahnke *et al* 2004 *Phys. Rev. Lett.* **93** 173401) while the lifetimes of the surface atoms differ significantly. Hence, the experimental lifetime can not purely be explained by the effect of the number of neighbours. We propose the possibility to investigate the transition from small clusters to the solid state by using the ICD electron spectra to distinguish between icosahedral and cuboctahedral cluster structures.

1. Introduction

The Interatomic Coulombic decay (ICD) is an electronic decay process of an atom or molecule with a sub-outer-valence vacancy involving atoms or molecules of the environment. The decay process is initiated by the creation of the vacancy, which can be achieved in different ways, out of which direct ionization, excitation, an Auger decay and radioactive decay are the most common ones. They are connected to different members of the family of ICD-like processes such as the electron transfer mediated decay (ETMD), the Resonance ICD, the ICD of multiply charged species like after an Auger decay and the classical ICD (see [1, 2] and references therein). In this paper the classical ICD of a sub-outer-valence vacancy in an atom or a molecule (a unit A) will be discussed. After creation of the vacancy in A, it is filled by an electron of the same unit and the excess energy (often called the energy of a virtual photon (vp) ω_{vp}) is transferred to a decay partner B, which subsequently gets ionized:

$$A^{*+} + B \rightarrow A^{+} + B^{+} + e^{-}_{\mathrm{ICD}}.$$

In the final state, the two units A and B are both positively charged, repell each other and thereby undergo a Coulomb explosion. This process was predicted theoretically [3], later the first experimental evidence was found in [4, 5] and the experimental prove was given by Jahnke *et al* [6]. Since then it has been studied in a multitude of different systems such as small and large rare gas clusters [7–15], clusters of small molecules [16–20], quantum dots [21], proteins [22], it is expected to play a role in DNA damage in radiation therapy [23] and may be used to destroy malign tissue [24, 25].

In order to undergo ICD and this process to be observable, two criteria have to be fulfilled: the energy and the coupling criterion. The energy criterion is a rephrasing of the energy conservation stating that a decay can only happen if the energy suffices. In case the energy of the doubly ionized final state is higher than the energy of the singly ionized initial state, the ICD is energetically forbidden. The coupling criterion requires the decay process to be sufficiently efficient to outperform other decay pathways such as radiative decay by emission of a photon or coupling to the nuclear degrees of freedom in molecules. The corresponding property is the decay width $\Gamma = \frac{\hbar}{\tau}$, which is inversely proportional to the lifetime τ and proportional to the decay rate $\frac{1}{\tau}$.

The ICD process was so far mostly discussed for the case of decay partners in the direct vicinity, because the decay with decay partners further away were considered to be negligible due to their decay width. Therefore, the decay was studied in clusters up to 13 neon atoms of equal interatomic distances considering the initial ionization of only the central atom and not the other ones [9]. The largest cluster had a cuboctahedral structure. In this study, a higher than linear dependence of the decay width on the number of neighbours was observed. A linear dependence would be expected for equal decay partners at equal distances from the initially ionized atom in the same environment. Since the decay width in the asymptotic limit shows an $1/\omega_{vp}^4$-behaviour on the energy of the vp, which is decreased for a stabilized final state, this additional feature can be related to the better energetic stabilization of the doubly ionized final state in larger clusters [26].

It was shown in earlier studies [15, 26–28] that decay pathways with decay partners at larger distances need to be included for larger systems for two reasons:

(i) In cluster structures more than one pair of units can consist of the same atom types and have the same interatomic distance. Hence, they are indistinguishable in the spectrum. Since the decay rate as well as the peak intensity is proportional to the number of such pairs, the peaks stemming from several pairs are favoured compared to other ones at similar distances. Therefore, peaks stemming from decays with distant decay partners can be visible in ICD spectra of clusters [15].

(ii) The opening of ICD-like decay channels depends on the interatomic distance, which is characteristic for every atom pair. A channel being closed at the distance to the most direct neighbours might be open for interaction partners at slightly larger distances. If this particular decay channel is more efficient than other decay channels being open for the decay with direct neighbours, it can still be visible in the spectrum or even outperform the slower decay mechanism and hence they have to be taken into account. We have shown this for the case of ICD versus the ETMD3 process in mixed ArXe clusters [26, 28].

Especially in the biological systems, in which ICD is discussed to play an important role [23–25] the DNA is surrounded by multiple moving water molecules which can act as decay partners. Therefore, understanding the effect of non-nearest neighbour decay will be crucial to study these systems. However, this feature of non-nearest neighbour ICD has so far not been addressed by itself and we will fill the gap in this paper.

For a test system we choose rare gas clusters. These are favourable for the investigation of basic features both from a theoretical and an experimental point of view. Their spherical symmetry and their very localized orbitals allow for an comparably easy theoretical description of the decay processes. The experimental techniques to produce rare gas clusters are well established via variety of experimental and theoretical studies [5, 29–31]. This makes these clusters a convenient target with controlled and predictable cluster conditions available at sufficient target densities for extended time periods as required in the here described experiments. At the same time, the structure of the clusters reveals an interesting matter of research. Small, ideal clusters exhibit an icosahedral structure while large clusters have a cuboctahedral structure, which infinitely extended, yields the solid state face-centered-cubic (fcc) structure. In the solid state, every single atom is surrounded by twelve other atoms in the same distance. Surface atoms or even atoms at edges and vertices are rare compared to the number of atoms in the bulk. However, in small clusters most atoms are surface atoms and are therefore surrounded by less than the optimal 12 atoms. In the icosahedral cluster structure the interatomic distances between different layers are shorter than between atoms of the same layer. Therefore, this structure is favourable in small clusters with a large surface-to-bulk ratio. Together with the structure change from icosahedral to cuboctahedral the clusters' properties gradually change towards those of solids and conductivity as well as magnetizability can be observed [32]. It is still unclear at which cluster size the favourable structure changes from an icosahedral to an cuboctahedral structure. Numbers in the range of 800–3000 atoms have been reported [33, 34]. We propose to use the ICD to be a possible tool to distinguish between icosahedral and cuboctahedral cluster structures using the different distance patterns in the cluster structures.

We will therefore first introduce the theoretical concepts in section 2, present the computational details in section 3, discuss the distance dependency of the ICD in general in section 4 and then discuss the NeNe ICD part of the ICD spectra of NeAr clusters [15] in section 5.1. Here we will discuss the peaks and their origin in detail and thereby raise the question, what a *nearest neighbour* is supposed to be. From our conclusions we propose the possibility to distinguish cluster structures of ideal icosahedral and cuboctahedral structures using ICD spectra in section 5.2.

2. Theoretical background

In order to simulate the ICD electron spectra for a given cluster structure, the kinetic energies of the ICD electrons E_{ICD} and the corresponding decay widths of all pairs have to be determined. The ICD electron energies

Table 1. Experimental values for the single ionization potentials [15] used for the estimation of the decay widths.

Indicator	Value
SIP(Ne2s)	47.75 eV
SIP(Ne2p)	21.10 eV
SIP(Ar3p)$_{c<3}$	15.40 eV
SIP(Ar3p)$_{c\geqslant 3}$	15.20 eV

are given by the differences between the initial state and the final state energies E_{in} and E_{fin}, respectively. The initial state energy is given by the single ionization potential (SIP) of the sub-valence electron of the entire system and the final state energy is given by the double ionization potential. In the asymptotic limit, which is a reasonably good approximation for weakly bound systems, the initial state energy is approximated by the SIP of the initially ionized unit X_{in} and the final state energy can be approximated by the sum over the SIPs of the electron donating unit X_{D} and the electron emitting unit X_{E} ionized in the final state as well as the Coulomb repulsion between two point charges at the interatomic distance R

$$E^{\beta}_{\mathrm{ICD}} = E^{\beta}_{\mathrm{in}} - E^{\beta}_{\mathrm{fin}}, \tag{1}$$

$$E_{\mathrm{in}} = \mathrm{SIP}(X_{\mathrm{in}}), \tag{2}$$

$$E^{\beta}_{\mathrm{fin}} = \mathrm{SIP}(X^{\beta}_{\mathrm{D}}) + \mathrm{SIP}(X^{\beta}_{\mathrm{E}}) + \frac{1}{R}. \tag{3}$$

Here, β denotes the selected decay channel.

Following Wentzel [35], Feshbach [36, 37] and Fano [38] the decay width is given by

$$\Gamma_{\beta}(E_{\mathrm{res}}) = 2\pi \; |\langle |\Phi_{\mathrm{in}}|H_{\mathrm{f}}|\chi_{\beta}|\rangle|^2. \tag{4}$$

Here, the bound and ionized initial state is described by $|\Phi_{\mathrm{in}}\rangle$ and the final continuum state of a particular decay channel β is given by $|\chi_{\beta}\rangle$. Its challenging description involving both bound and continuum states can amongst others be achieved by the FanoADC-Stieltjes approach, where a subset of the 2-hole-1-particle (2h1p) functions within the algebraic diagrammatic construction (ADC) are used to mimic the final state function $|\chi_{\beta}\rangle$. By these means calculated discrete energies and corresponding transitions moments are then used to construct a continuous function, which is evaluated at the resonance energy approximated by the single ionization potential corresponding to the initial state E_{in}. For a more detailed description of the method and comparison to other approaches see [39, 40] and references therein.

3. Computational details

The cluster structures used were constructed to have an ideal icosahedral or fcc geometry with optional additional incomplete outermost shells. These are based on the van der Waals radii for neon $r_{\mathrm{Ne}} = 1.54$ Å and argon $r_{\mathrm{Ar}} = 1.88$ Å [41]. In case of the NeAr clusters two of those cluster structures from [15], where the theoretical and experimental argon content in the cluster, the NeAr-ICD to total ICD ratio and the peak position of the NeAr-ICD peak matched best for a given manifold (set) of clusters produced under certain experimental conditions, have been chosen. These are $C_{\mathrm{Ar}} = 3$, $C_{\mathrm{Ne}} = 1$, $S_{\mathrm{Ne}} = 7$ for set 3 and $C_{\mathrm{Ar}} = 2$, $C_{\mathrm{Ne}} = 1$, $S_{\mathrm{Ne}} = 13$ for set 5 where we used the same nomenclature as in [15]. Hence, C_{Ar} denotes the edge length of the argon core, C_{Ne} denotes the number of complete neon shells around the argon core and S_{Ne} denotes the number of triangular surfaces additionally covered by neon atoms.

The calculations to obtain the ICD electron spectra of all cluster structures were performed with the program HARDRoC [42] based on the decomposition of the cluster into pairs. Every pair with the same distance is treated equally. This includes the assumption that every neon atom is ionized with the same probability [15, 43]. It uses experimental ionization energies shown in table 1 and curves fitted to the decay width of the NeNe ICD of [10] and the NeAr decay widths of [15]. These fitted curves yield lifetimes $\tau = \frac{\hbar}{\Gamma}$ at the corresponding equilibrium distances of $\tau_{\mathrm{NeNe}} = 60$ fs and $\tau_{\mathrm{NeAr}} = 44$ fs.

4. Decay with decay partners at different distances

To fully understand the spectra of clusters with several possible initially ionized atoms with multiple decay partners it is necessary to understand the properties of the decay of a single pair of atoms. As can be seen from

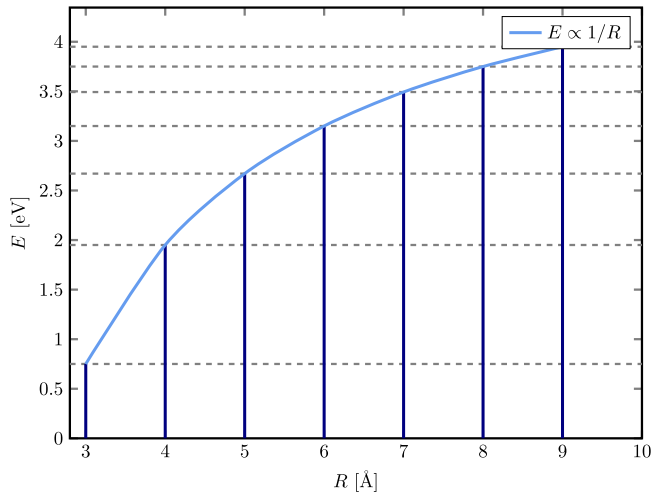

Figure 1. Kinetic energy of the ICD electron depending on the interatomic distance of the two atoms in an isolated pair involved in the decay within the asymptotic approximation. The kinetic energy shows a $1/R$ behaviour and hence distance changes at small distances lead to larger changes in the kinetic energy than at larger distances.

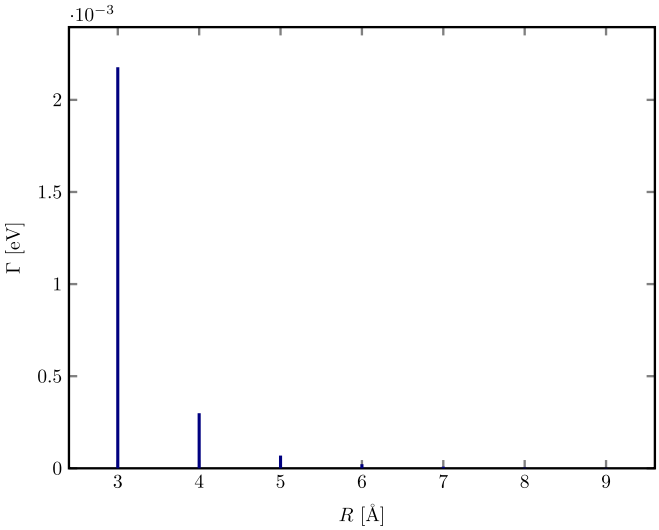

Figure 2. Decay widths for different interatomic distances following an asymptotic $1/R^6$-behaviour. For distances larger than twice the shortest distance considered the peaks are not visible in this plot.

equations (1)–(3), the kinetic energy of the ICD electron follows an $1/R$-behaviour shown in figure 1 for the case of a neon dimer at different distances.

From this diagram it can already be seen that the kinetic energies stemming from equidistant peaks of 3, 4, 5, … , 9 Å are not equidistant in their energy difference but rather decrease for an increasing interatomic distance.

The corresponding decay widths Γ depending on the interatomic distance are shown in figure 2. They show an asymptotic $1/R^6$-behaviour such that the decay widths from an interatomic distance of 7 Å on are too small to be seen in the figure. This means that in case of a neon dimer with an internuclear distance of 3 Å, a decay with one decay partner at twice the internuclear distance of the neon dimer is very unlikely, but that interactions with decay partners at shorter distances can not in general be neglected.

A similar picture is given by the hypothetical ICD-electron spectrum for decay partners at distances of 3, 4, …, 9 Å shown in figure 3. Here, the kinetic energy of the ICD electron is depicted on the abscissa while the decay width Γ is plotted on the ordinate. Since the decay width is proportional to the decay rate and hence the decay probability, these spectra can directly be compared to experimental ICD electron spectra.

The first and dominant peak stems from the decay with a decay partner at a distance of 3 Å. The energy distance to the next peak stemming from a decay with a decay partner with an internuclear distance of 4 Å is found at a 1.20 eV higher kinetic energy and the energy difference to the next peak stemming from a 5 Å distant

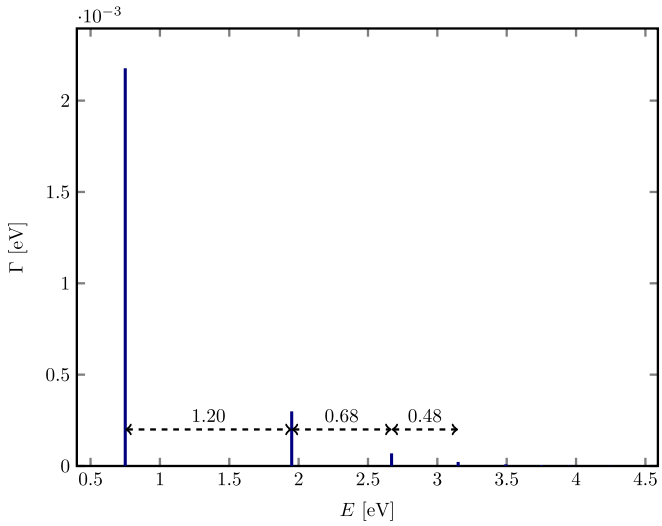

Figure 3. ICD electron spectrum for interaction partner distances of 3 , 4 , 5 , … ,9 Å. The energy difference between equidistant interaction partners decreases with increasing distance. For the case of Ne_2 pairs these energy differences between the peaks stemming from different interatomic distances are given by: 3 Å, 4 Å → 1.20 eV, 4 Å, 5 Å → 0.68 eV and 5 Å, 6 Å → 0.48 eV. This means that the spectrum is better resolved for smaller distances and that small distance changes like vibrations will mainly affect this lower energy part of the spectrum.

decay partner is further 0.68 eV higher. The increase of kinetic energy of the ICD electron is caused by a decrease of Coulomb repulsion between the interaction partners in the final state and therefore, the additional excess in energy is converted into kinetic energy of the emitted ICD electron. The energy difference between the peaks shown in figure 3 decreases with an increasing distance of decay partners and at the same time the kinetic energy of the ICD electron. This means that for small interatomic distances and comparably low kinetic energies of the ICD electron, the energy spectrum has a higher resolution of the interatomic distances. Therefore, a peak structure might be visible for the decay with nearest neighbours (or the closest atoms with energetically allowed decay channels) but not necessarily for all different kinds of interaction partners at larger distances.

5. ICD in clusters

5.1. NeAr clusters

After ionization from the Ne2s, a heteronuclear NeAr cluster can decay via two competing pathways:

$$\mathrm{Ne}(2s^{-1}) + \mathrm{Ne} \rightarrow \mathrm{Ne}(2p^{1}) + \mathrm{Ne}(2p^{-1}) + e^{-}_{\mathrm{ICD}},$$
$$\mathrm{Ne}(2s^{-1}) + \mathrm{Ar} \rightarrow \mathrm{Ne}(2p^{-1}) + \mathrm{Ar}(3p^{-1}) + e^{-}_{\mathrm{ICD}}$$

in which the excess energy gained by filling the Ne2s vacancy is transferred to either another neon atom or to an argon atom. Since the lifetimes of the NeNe-ICD and the NeAr-ICD are of the same order of magnitude, both are visible in the secondary electron spectrum (see figure 2 of [15]). The two signals are well separated in energy and both consist of a main peak and a shoulder at higher kinetic energies of the ICD electron. We earlier showed a clear geometry dependence of peak intensity relation of the NeNe-ICD and NeAr-ICD and utilized this property to determine the structure of heteroatomic rare gas clusters [15].

The peak structure of one main peak and a shoulder at higher energies has been discussed for the NeAr before. Theoretical investigations indicate that the shape might be caused by different vibrational levels of the NeAr dimer ($v = 0, 1, 2$) being populated prior to the initial ionization, because the calculated lifetimes of the intermediate states were too short to allow for nuclear dynamics [44]. There, the ratio of the population of the three vibrational levels 10:5:4 was chosen to yield a spectrum close to the experimental spectrum of NeAr clusters. However, recent experimental results of the ICD in the NeAr dimer show a symmetric peak without a shoulder [45]. In order to explain this, the authors assume a bond contraction of the $Ne^{+}Ar$ to happen prior to the decay. This nuclear rearrangement would contradict the theoretically predicted lifetime of the system and they therefore propose the prior value to be wrong and give an estimate for a higher lifetime. We would like to emphasize the possibility that mainly the vibrational ground state was populated at the temperatures at which the experiment was conducted and that the theoretically predicted lifetimes are correct. Since the shoulder appears in the spectrum of clusters only and not in the dimer spectra, we interpret these experimental results of

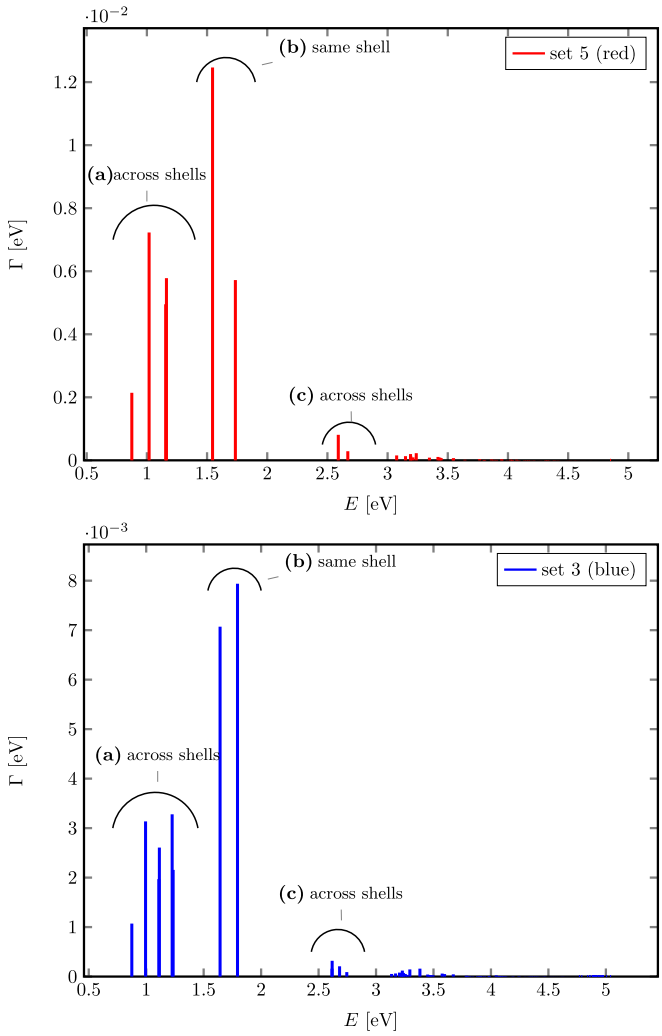

Figure 4. ICD spectra for the NeNe-ICD part of the structures of set 3 and set 5 of the NeAr clusters in [15] plotted as stick spectra. The different peak groups resemble different pair types within the NeAr clusters. The lowest energy peaks ((a)) refer to nearest neighbours of different shells, the peak group (b) refers to nearest neighbours within one shell and the peak group (c) refers to next-nearest neighbours between adjacent shells. The other peaks contain both peaks stemming from pairs within the same shell as well as pairs consisting of atoms of different shells. In this representation the contribution of the peaks around 3 eV is easily underestimated. After folding the spectrum with many close lying small peaks they will add up to yield a visible peak or shoulder (compare [15]).

the dimer to confirm our findings, that the shoulder stems from ICD with interaction partners of the next shell [15].

In the neon dimer several vibrational states of the ionized initial state are involved in the decay [7]. It has furthermore been shown, that the experimentally determined lifetime of $\tau_{\mathrm{NeNe}} = 150 \pm 50$ fs [46] is only in agreement with those theoretical lifetime calculations that explicitly include nuclear dynamics of the intermediate state [47]. However, the early lifetime measurements in neon clusters with a mean cluster size of $< N > = 900$ atoms show a lifetime of 30 fs for surface atoms and 6 fs for bulk atoms. This lifetime decrease is caused by the possibility to decay with several decay partners. Nuclear dynamics occur in the range of tens of femtoseconds in the dimer. Additionally, the driving force for a bond contraction after the initial ionization is higher in dimers than in clusters, where one bond contraction usually leads to several bond elongations. Therefore, we consider the influence of nuclear dynamics on the lifetime to be sufficiently small to be able to neglect them in clusters in a first description [5, 9]. In the following, we will focus on the NeNe-ICD part of the ICD electron spectra of the NeAr clusters and analyze them in more detail.

In figure 4 the ICD electron spectra for the NeNe-ICD part of heterogeneous clusters are shown as stick spectra for set 3 and set 5. Hereby, we stick to the naming and the color code of [15]. Both spectra exhibit a similar pattern of peak groups. The groups are found around 1.0 eV (group (a)), around 1.7 eV (group (b)), around 2.6 eV (group (c)) and from 3 to 4 eV. The peak groups can be assigned to atom pairs within the cluster. For group (a) the peaks stem from decays between two nearest neighbour atoms of two different shells, while group (b) stems from the decay partners being nearest neighbours in the same shell. Group (c) can be assigned to

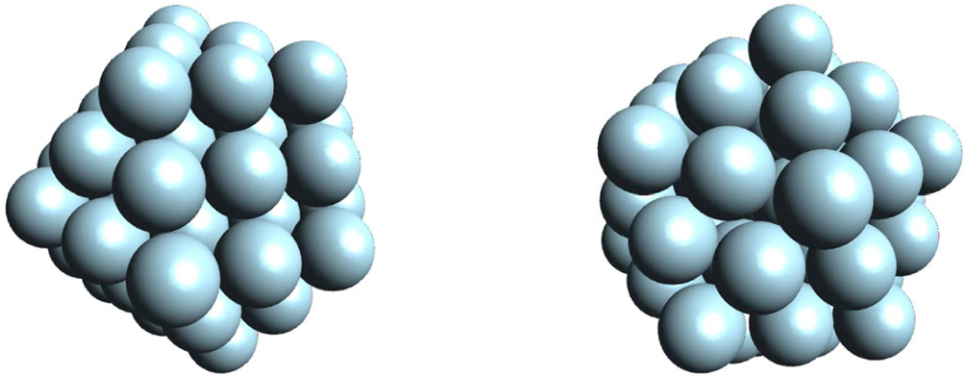

Figure 5. Cluster structures of the 55 atom Ne clusters with cuboctahedral structure (left) and icosahedral structure (right).

Table 2. Calculated decay widths and lifetimes of bulk and surface atoms for icosahedral and cuboctahedral clusters of 55 and 923 atoms.

		Atoms	Γ (meV)	τ (fs)
Icosahedral	Bulk	55	125	5.3
	Surface	55	67	9.8
	Bulk	923	126	5.2
	Surface	923	81	8.1
Cuboctahedral	Bulk	55	140	4.7
	Surface	55	78	8.4
	Bulk	923	147	4.5
	Surface	923	95	7.0

non-nearest neighbours in adjacent shells and the other peaks stem from a mixture of pairs which cannot unambigiously be categorized because different kinds of peaks intersect each other.

Obviously, the peak groups have a fine structure which originates from different positions of the decay partners within a shell (face, egde or vertex). For the investigated ideal icosahedral structures, these pairs of group (a) are from low to high kinetic energies: vertex–vertex, edge–edge, edge–face and face–face. Due to vibrational broadening of the peaks the experimental observation of this fine structure is unlikely in neon clusters.

Concluding these findings, there is not neccessarily only one kind of nearest neighbours in clusters. Even the next-nearest neighbours are closer to twice the interatomic distance of the closest pair with an open decay channel. Therefore, also non-nearest decay partners need to be taken into account in order to simulate ICD spectra of clusters. It can be considered safe to neglect decay partners at sufficiently larger distances than twice the closest interatomic distance between decay partners with open channels.

5.2. Neon clusters: icosahedral versus cuboctahedral structure of clusters

We study two cluster structures (shown in figure 5), where one has an idealized icosahedral and the other one has an idealized cuboctahedral structure for clusters of both 55 and 923 atoms. They hence consist of 13 (561) core and 42 (362) surface atoms.

It was predicted theoretically and proven experimentally that the lifetimes of ionized bulk atoms is shorter than of ionized surface atoms due to the smaller number of direct neighbours of surface atoms [5, 9]. The experimentally determined lifetimes are $\tau_{\mathrm{surf}} = 30$ fs and $\tau_{\mathrm{bulk}} = 6 \pm 1$ fs [5]. For our 55 and 923 atom cluster the decay widths and lifetimes are listed in table 2.

In all cases, our results confirm the shorter lifetimes of the bulk atoms compared to the surface atoms. Both for the icosahedral and for the cuboctahedral cluster structure the lifetime of the bulk atoms is almost independent of the cluster size and the difference is maximum 0.2 fs. This can be explained by the very similar environments of bulk atoms in smaller and larger clusters. The lifetimes of the surface atoms however are smaller for the larger cluster sizes. In small clusters, the number of face surface atoms is small compared to the number of edge and vertex atoms in the surface. The larger the clusters are, the larger is the relative number of the surface atoms. These surface atoms in face positions have more direct neighbours than atoms in vertex

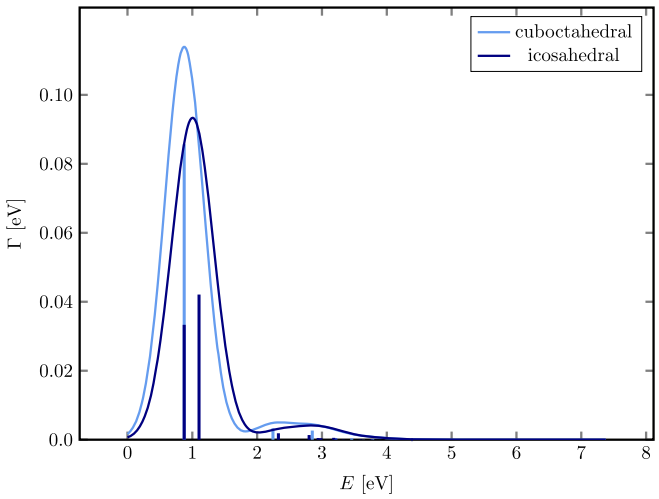

Figure 6. ICD spectra of pure neon clusters consisting of 55 atoms in icosahedral and cuboctahedral structure. In clusters with an ideal cuboctahedral structure all interatomic distances are the same and hence only one peak for each shell around any atom in the cluster is to be expected. In ideal icosahedral clusters the interatomic distances between atoms within the same shell and between atoms in neighbouring atoms are different. Therefore two peaks for interactions partners at different distances can be expected. This feature might help to experimentally identify the underlying structure of clusters.

positions. Therefore, our estimated lifetime of the average surface atoms in the small clusters should be slightly larger than in larger clusters.

For both the icosahedral and the cuboctahedral cluster structures the lifetimes of the bulk atoms are in excellent agreement with experiment. However, the theoretical lifetimes of the surface atoms are significantly smaller than the experimental lifetime. Assuming that the experimental lifetimes are correct, we have to consider three error sources: (1) the nuclear motion excluded in our approach, (2) different cluster structures, and (3) a different stabilization of charges between the inner-valence ionized and the outer-valence ionized atom compared to the bulk.

Cluster structures with larger interatomic distances of the surface atoms between each other and the core atoms would explain the higher experimental lifetimes of the surface atoms. These could be caused by non-ideal structures due to the clusters' temperature.

It remains to discuss the influence of the different charge stabilizations of inner- and outer-valence vacancies. The decay width is proportional to $\frac{1}{\omega_{\mathrm{vp}}^4}$ where the energy of the vp is given by

$$\omega_{\mathrm{vp}} = \mathrm{SIP}(X_{\mathrm{in}}) - \mathrm{SIP}(X_{\mathrm{D}}). \tag{5}$$

If the stabilization difference of the inner-valence vacancy between the bulk and the surface atoms is larger than the corresponding difference of the outer-valence vacancy, the transferred energy is increased in case of the surface atoms ($\omega_{\mathrm{vp,surf}} > \omega_{\mathrm{vp,bulk}}$). As a consequence, the decay width is decreased and the lifetime is increased. Unfortunately, only the initial state energy differences are to be found in the literature [5]. Hence, a validation of this cause is currently not possible.

Before discussing the ICD spectra of the icosahedral and cuboctahedral cluster structures shown in figure 6, we would like to recall that clusters with an icosahedral structure have shorter interatomic distances between shells than within the same shell. In terms of the ICD, different groups of nearest neighbours exist, one within the same shell and one between adjacent shells. This is characteristic for icosahedral cluster structures. Cuboctahedral cluster structures on the other hand are characterized by only one interatomic distance. Therefore, icosahedral cluster structures should be distinguishable from cuboctahedral clusters by the number of peaks, which can be seen in figure 6.

Two experimental ICD electron spectra of clusters with a mean cluster size $<N>$ of 70 and 209 atoms are available in the literature [4, 48]. The first experimental spectrum for clusters with $<N> = 70$ shows a very broad ICD electron peak without an unambiguously assignable peak structure, whereas the later results show a main peak of ICD electrons and a smaller peak at slightly higher kinetic energies (at around 3 eV) that was not even assigned to be an ICD peak in the original work. This peak corresponds to the decay with non-nearest neighbours in the adjacent shell. However, a further peak structure is not visible.

Whether or not the cluster structures would be distinguishable in experiment will depend on the vibrational broadening of the peaks, the experimental resolution and difference of the interatomic distances and hence the energy difference of the peaks in the spectrum of the icosahedral structure. In this proof-of-principle discussion

we chose neon clusters for comparison with experiment but for the distinction of cluster structures it might be recommendable to choose atoms with larger internuclear distances in clusters.

6. Summary

We have discussed two of the three aspects one needs to take into account to simulate the ICD spectrum of rare gas clusters properly. Due to the nature of clusters, a neon atom ionized in the inner-valence will have several decay partners at different distances. The larger the interatomic distance is the higher is the kinetic energy of the ICD electrons which will yield a multitude of peaks in the spectrum. These are then weighted by the decay width, which depends on the interatomic distance of the decay partners but also needs to be scaled by the number of pairs of the same distance. The manifold of all different decay events will then yield the spectrum.

When applying these aspects to cluster structures, one finds that not only the nearest neighbours contribute to the spectrum, but several other decay partners do as well. Decay partners until a distance of at least twice the distance of the clostest decay partners should be taken into account. In clusters with an icosahedral cluster structure this is especially important because the smallest interatomic distance between atoms of the same and atoms of different layers is different, but both distances are comparable. This leads to a different number of peaks in the spectra which might help to distinguish between clusters of icosahedral and cuboctahedral cluster structure.

While the theoretical lifetime of the bulk atoms show an excellent agreement with experiment, the lifetimes of the surface atoms differ significantly. This deviation might be caused by different static cluster structures than taken into account in this work, by different energetic stabilization of charges or by nuclear dynamics. Which of these reasons explains the experiment can not be determined at the moment. Experimentally determined photoelectron spectra of the outer valence of high resolution in neon clusters would help to solve this puzzle.

Acknowledgments

Funding from the Research Council of Norway through a Centre of Excellence Grant (Grant No. 179568/V30) is gratefully acknowledged.

References

[1] Hergenhahn U 2011 Interatomic and intermolecular coulombic decay: the early years *J. Electron Spectrosc. Relat. Phenom* **184** 78
[2] Jahnke T 2015 Interatomic and intermolecular Coulombic decay: the coming of age story *J. Phys. B: At. Mol. Opt. Phys.* **48** 082001
[3] Cederbaum L S, Zobeley J and Tarantelli F 1997 Giant intermolecular decay and fragmentation of clusters *Phys. Rev. Lett.* **79** 4778
[4] Marburger S, Kugeler O, Hergenhahn U and Möller T 2003 Experimental evidence for interatomic coulombic decay in Ne clusters *Phys. Rev. Lett.* **90** 203401
[5] Öhrwall G *et al* 2004 Femtosecond interatomic coulombic decay in free neon clusters: large lifetime differences between surface and bulk *Phys. Rev. Lett.* **93** 173401
[6] Jahnke T *et al* 2004 Experimental observation of interatomic Coulombic decay in neon dimers *Phys. Rev. Lett.* **93** 163401
[7] Santra R, Zobeley J, Cederbaum L S and Moiseyev N 2000 Interatomic Coulombic decay in van der Waals clusters and impact of nuclear motion *Phys. Rev. Lett.* **85** 4490
[8] Santra R, Zobeley J, Cederbaum L S and Tarantelli F 2001 Intermolecular Coulombic decay of clusters *J. Electron Spectrosc. Relat. Phenom.* **41** 114–6
[9] Santra R, Zobeley J and Cederbaum L S 2001 Electronic decay of valence holes in clusters and condensed matter *Phys. Rev.* B **64** 245104
[10] Averbukh V and Cederbaum L S 2006 Calculation of interatomic decay widths of vacancy states delocalized due to inversion symmetry *J. Chem. Phys.* **125** 094107
[11] Lundwall M *et al* 2007 Self-assembled heterogeneous argon/neon core-shell clusters studied by photoelectron spectroscopy *J. Chem. Phys.* **126** 214706
[12] Jahnke T *et al* 2010 Ultrafast energy transfer between water molecules *Nat. Phys.* **6** 139
[13] Förstel M, Arion T and Hergenhahn U 2013 Measuring the efficiency of interatomic Coulombic decay in Ne clusters *J. Electron Spectrosc. Relat. Phenom.* **191** 16
[14] Mucke M, Arion T, Förstel M, Lischke T and Hergenhahn U 2015 Competition of inelastic electron scattering and interatomic Coulombic decay in Ne clusters *J. Electron Spectrosc. Relat. Phenom.* **200** 232
[15] Fasshauer E, Förstel M, Pallmann S, Pernpointner M and Hergenhahn U 2014 Using ICD for structure analysis of clusters: a case study on coexpanded Ne–Ar clusters *New J. Phys.* **16** 103026
[16] Zobeley J, Cederbaum L S and Tarantelli F 1998 Highly excited electronic states of molecular clusters and their decay *J. Chem. Phys.* **108** 9737
[17] Pernpointner M, Knecht S and Cederbaum L S 2006 Ionization spectra and electronic decay in small iodide clusters: fully relativistic results *J. Chem. Phys.* **125** 034309
[18] Müller I B and Cederbaum L S 2006 Ionization and double ionization of small water clusters *J. Chem. Phys.* **125** 204305
[19] Kryzhevoi N V and Cederbaum L S 2011 Using pH value to control intermolecular electronic decay *Angew. Chem., Int. Ed.* **50** 1306
[20] Ghosh A, Pal S and Vaval N 2013 Study of interatomic Coulombic decay of Ne(H2O)n ($n = 1, 3$) clusters using equation-of-motion coupled-cluster method *J. Chem. Phys.* **139** 064112
[21] Bande A 2013 Electron dynamics of interatomic coulombic decay in quantum dots induced by a laser field *J. Chem. Phys.* **138** 214104

[22] Harbach P H P, Schneider M, Faraji S and Dreuw A 2013 Intermolecular coulombic decay in biology: the initial electron detachment from FADH-in DNA photolyases *J. Phys. Chem. Lett.* **4** 943
[23] Alizadeh E, Orlando T M and Sanche L 2015 Biomolecular damage induced by ionizing radiation: the direct and indirect effects of low-energy electrons on DNA *Annu. Rev. Phys. Chem.* **66** 379
[24] Gokhberg K, Kolorenč P, Kuleff A I and Cederbaum L S 2014 Site- and energy-selective slow-electron production through intermolecular Coulombic decay *Nature* **505** 661
[25] Trinter F *et al* 2014 Resonant Auger decay driving intermolecular Coulombic decay in molecular dimers *Nature* **505** 664
[26] Fasshauer E, Pernpointner M and Gokhberg K 2013 Interatomic decay of inner-valence ionized states in ArXe clusters: relativistic approach *J. Chem. Phys.* **138** 014305
[27] Kryzhevoi N V, Averbukh V and Cederbaum L S 2007 High activity of helium droplets following ionisation of systems inside those droplets *Phys. Rev.* B **76** 094513
[28] Fasshauer E, Förstel M, Mücke M, Pernpointner M and Hergenhahn U in preparation
[29] Hagena O F and Obert W 1972 Cluster formation in expanding supersonic jets: effect of pressure, temperature, nozzle size, and test gas *J. Chem. Phys.* **56** 1793–802
[30] Hagena O F 1981 Nucleation and growth of clusters in expanding nozzle flows *Surf. Sci.* **106** 101
[31] Hagena O F 1987 Condensation in free jets: comparison of rare gases and metals *Z. Phys.* D **4** 291
[32] Benfield R E 1992 Mean coordination numbers and the non-metal-metal transition in clusters *J. Chem. Soc. Faraday Trans.* **88** 1107
[33] Hartke B 2002 Structural transitions in clusters *Angew. Chem., Int. Ed.* **41** 1468
[34] Pahl E, Calvo F, Koči L and Schwerdtfeger P 2008 Accurate melting temperatures for neon and argon from ab initio Monte Carlo simulations *Angew. Chem., Int. Ed.* **47** 8207
[35] Wentzel G 1927 Über strahlungslose quantensprünge *Z. Physik.* **43** 524
[36] Feshbach H 1958 Unified theory of nuclear reactions *Ann. Phys.* **5** 357
[37] Feshbach H 1962 A unified theory of nuclear reactions: II *Ann. Phys* **19** 287
[38] Fano U 1961 Effects of configuration interaction on intensities and phase shifts *Phys. Rev.* **124** 1866–78
[39] Averbukh V and Cederbaum L S 2005 Ab initio calculation of interatomic decay rates by a combination of the fano ansatz, Green's-function methods, and the stieltjes imaging technique *J. Chem. Phys.* **123** 204107
[40] Fasshauer E, Kolorenč P and Pernpointner M 2015 Relativistic decay widths of autoionization processes: the relativistic fanoadc-stieltjes method *J. Chem. Phys.* **142** 144106
[41] Bondi A 1964 van der Waals volumes and radii *J. Phys. Chem.* **68** 441
[42] Fasshauer E 2013 HARDRoC, hunting asymptotic relativistic decay rates of clusters (http://www.pci.uni-heidelberg.de/tc/usr/elke/hardroc/html/main.html)
[43] Fasshauer E 2014 Investigation of relativistic effects in electronic decay processes in small and large noble gas clusters by ab initio and new simulation approaches *PhD thesis* University of Heidelberg
[44] Scheit S, Averbukh V, Meyer H-D, Zobeley J and Cederbaum L S 2006 Interatomic Coulombic decay in a heteroatomic rare gas cluster *J. Chem. Phys.* **124** 154305
[45] O'Keeffe P *et al* 2014 Experimental investigation of the interatomic Coulombic decay in NeAr dimers *Phys. Rev.* A **90** 042508
[46] Schnorr K *et al* 2013 Time-resolved measurement of interatomic Coulombic decay in Ne_2 *Phys. Rev. Lett.* **111** 093402
[47] Schnorr K *et al* 2015 Time-resolved study of ICD in Ne dimers using FEL radiation *J. Electron Spectrosc. Relat. Phenom.* **204** 245
[48] Barth S, Marburger S, Kugeler O, Ulrich V, Joshi S, Bradshaw A M and Hergenhahn U 2006 The efficiency of interatomic Coulombic decay in Ne clusters *Chem. Phys.* **329** 246